

# Cardiovascular Risk Detection in Sleep Apnea Patients from Pulse Photoplethysmography Waveform

Dorien Huysmans<sup>1</sup>, Pascal Borzée<sup>2</sup>, Bertien Buyse<sup>2</sup>,  
Dries Testelmans<sup>2</sup>, Sabine Van Huffel<sup>1</sup>, Carolina Varon<sup>1</sup>

<sup>1</sup> STADIUS Center for Dynamical Systems, Signal Processing and Data Analytics, Department of Electrical Engineering (ESAT), KU Leuven, Leuven, Belgium  
<sup>2</sup> Department of Pneumology, UZ Leuven, Leuven, Belgium

## Abstract

*Obstructive sleep apnea is often associated with cardiovascular diseases (CVD). Early CVD detection would enhance patient selection for diagnosis and treatment prioritization, to avert development of aggravating CVD. Therefore, the aim of this study is to find markers of CVD risk factors in the pulse photoplethysmography signal, as this enables wearable assessment. To avoid the influence of apneic events on the PPG signal and the requirement to retain the correct sensor positioning for a full night, a method based on wakefulness was investigated. From the PPG, the wake period in the evening before falling asleep and the wake period after waking up in the morning were extracted. A set of 148 features characterized the PPG waveform, using window sizes of 5s to 85s in steps of 5s. A stratified 10-fold cross validation was repeated 100 times for feature selection and CVD classification of 78 subjects. The mean diastolic width at 10% of pulse amplitude (mean DT 10%) was overall the most distinctive feature for CVD risk detection as it showed a significant decrease for CVD patients. Pre-sleep pulse width features extracted over 45s resulted in  $\kappa = 0.46$ , a sensitivity of 72.1% and specificity of 74.3%. Overall, mean DT 10% contained CVD risk information, but the result requires further validation on larger datasets and wearable sensors.*

## 1. Introduction

Obstructive sleep apnea (OSA) is the most common sleep related breathing disorder, estimated to affect one billion people worldwide. It is characterized by events of breathing disturbances causing hypoxemia and arousals from sleep. Consequently, OSA is a recognized risk factor for excessive daytime sleepiness, hypertension and cardiovascular diseases (CVD). However, many patients remain undiagnosed. One of the reasons is the limited hospital capacity for performing polysomnography (PSG). Therefore, it is desired to prioritize patients for sleep apnea diagnosis and treatment, in order to avert development of aggravating CVD. To allow a wearable and ambulatory assessment, the objective of this study was to investigate the pulse photo-

plethysmography (PPG) signal of suspected OSA patients to find CVD risk markers.

The PPG measures the variation of light absorption related to the blood pulse wave and is typically acquired by a finger-worn device. It is already a standard sensor in ambulatory polygraphy and has been implemented in consumer electronics as well, such as smartwatches. Moreover, to avoid the influence of apneic events on the PPG signal and the requirement to retain the correct sensor positioning for a full night, a method based on wakefulness and very short term recordings is beneficial.

To support the idea, it is known that OSA alters the cardiovascular condition of a patient, including during daytime. This cardiovascular change can be measured by the heart rate variability (HRV) and is found to be reduced in OSA patients. The primary cause for this reduction is the patient's sympathetic overactivity, both acutely during apneic events and chronically during daytime [1]. However, these studies were based on analysis of ECG data and not on PPG data. Although high correlation has been observed between HRV indices derived from ECG and PPG, results were only valid for young healthy adults and deviating results were seen for OSA patients [1]. Therefore, HRV analysis cannot be directly translated to PPG data.

On the other hand, relations between blood pressure values, vascular tone and the PPG wave morphology was shown by several studies [2–4]. However, only a few studies derived the CVD risk level based on PPG [5]. Moreover, this is the first study that explores markers of CVD risk in the PPG signal of OSA patients during wakefulness.

## 2. Materials and Methods

### 2.1. Data

The dataset comprised finger PPG recordings from polysomnography (PSG) and information on hypertension, hyperlipidemia and diabetes of 78 patients with suspected sleep apnea. These patients were referred to the sleep laboratory of the University Hospitals Leuven (UZ Leuven) for a diagnostic PSG. The collection of data was approved by the ethical committee of UZ Leuven (S60319) and all

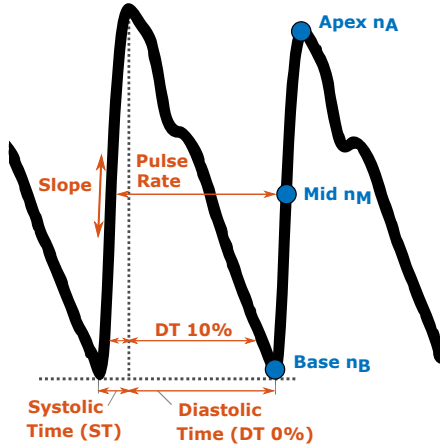


Figure 1: PPG characteristic points and descriptors.

patients signed an informed consent. From the PSG, the finger PPG, the room light sensor data, and the sleep annotations were extracted. The wake period before and after sleep was extracted. The first wake period started when the lights of the room were switched off until the patient fell asleep, which was derived from the sleep annotations. The second wake period started when the patient woke up, and did not fall asleep again, until the lights were switched on. Both periods had a minimal duration of 5 min.

## 2.2. Feature Extraction

The PPG signals were band-pass filtered between 0.3 Hz and 15 Hz. These frequencies were chosen to remove baseline wander and high-frequency noise, while retaining the necessary frequency content for detailed PPG waveform analysis. Then, delineation of the PPG pulses was performed as in [6] and consists of two steps. First, a differentiator filter was applied on the signal to accentuate the slopes. Second, an adaptive threshold was used to search peaks in the filtered signal, defining the apex point  $n_{A_t}$  of the PPG wave at time point  $t$  (see figure 1). In a window of 0.3s before  $n_{A_t}$ , the minimal pulse amplitude defined the basal  $n_{B_t}$  point. The mid-point  $n_{M_t}$  was at 50% of the amplitude maximum and is considered as a more robust point compared to  $n_{A_t}$  [6].

A set of descriptors was derived to extract time and frequency information of successive PPG waves, as well as to characterize the morphology of the PPG wave. A high quality PPG wave of a healthy person can be characterized by a systolic peak, dicrotic notch and diastolic peak. However, this wave shape can deviate from its model due to pathological conditions, signal quality or sensor location. Often, only the systolic peak can be detected. Therefore, descriptors in this study were based on basal and apex points, to account for different recording conditions.

Every PPG wave was defined by a total of 74 descriptors. An overview of these descriptors is given in Table 1. The descriptors could be divided in the following three categories.

Table 1: Overview of extracted descriptors.

#	Descriptor	Source
1	Pulse rate variability	[7]
3	Low frequency (LF, 0.04-0.15 Hz) power	[8]
	High frequency (HF, 0.15-0.4 Hz) power	
	LF/HF	
1	Slope transit time	[7]
1	Pulse width	[7]
2	Systolic time (ST), Diastolic time (DT)	[2]
36	DT, DT + ST and DT / ST	[4]
	at [10, 25, 33, 50, 66, 75]% pulse amplitude	
	unnormalized or normalized by heart rate	
1	Pulse area variability	[7]
1	Slope	[7]
4	Subareas unnormalized	
12	Subareas normalized by amplitude	
12	Subareas normalized by heart rate	

**Beat interval:** A first set of descriptors was based on the time interval between two heart beats or the difference between  $n_{M_{t+1}}$  and  $n_{M_t}$ . One descriptor was the pulse rate variability (PRV) [7]. Three other descriptors were derived from the instantaneous heart rate (IHR). At every heart beat, the low frequency (LF, 0.04-0.15 Hz) power, the high frequency (HF, 0.15-0.4 Hz) power and the LF/HF ratio were calculated [8].

**Time:** The second set described the time interval between characteristic points within the PPG wave. The first parameters were the slope transit time and pulse width, as defined by [7]. Other descriptors were the systolic (ST,  $n_{B_t}$  to  $n_{A_t}$ ) and diastolic time (DT,  $n_{A_t}$  to  $n_{B_{t+1}}$ ) [2], and variations of ST and DT. These variations were the DT, DT + ST and DT / ST extracted at different percentiles of the pulse amplitude (10%, 25%, 33%, 50%, 66%, 75%) [4]. Furthermore, these ratios were either applied as such, or normalized by the IHR as this had an influence on pulse widths.

**Amplitude:** The last set quantifies the amplitude of the PPG wave. These descriptors correspond to the pulse area variability (PAV, amplitude difference between  $n_{B_t}$  and  $n_{A_t}$ ), upslope and area between two consecutive basal points [7]. Furthermore, four subareas were defined:  $n_{B_t}$  to  $n_{M_t}$ ,  $n_{B_t}$  to  $n_{A_t}$ ,  $n_{B_t}$  to  $n_{B_{t+1}}$  and  $n_{A_t}$  to  $n_{B_{t+1}}$ , from which the baseline amplitude at  $n_{B_t}$  was subtracted. Thereafter, the subarea was either normalized as  $a_{norm} = (a - \min) / (\max - \min)$  or  $a_{norm} / \overline{IHR} = (a - \min) / (\overline{IHR})$ , with min and max respectively the minimal and maximal value of the normalization window, and  $\overline{IHR}$  the average IHR of the normalization window. This normalization window comprised either one, three or five waves, centered at the wave for which the descriptor was calculated. The described beat-interval, time and amplitude descriptors were calculated at each PPG wave. For further

analysis, continuous time series of evenly sampled descriptor values were required. As such, the PPG wave descriptors were resampled to 4 Hz, resulting in 74 time series. These were subsequently segmented in non-overlapping windows of fixed length. The mean and standard deviation (SD) were calculated over every window, resulting in two distributions of mean and SD values per descriptor. Finally, the 50<sup>th</sup> percentile of the mean distribution, on the one hand, and of the SD distribution, on the other hand, defined two aggregated feature values,  $F_{\text{mean}}$  and  $F_{\text{SD}}$ , respectively. The analysis was carried out in parallel using window sizes of 5s, 15s, 25s, 35s, 45s, 55s, 65s, 75s and 85s. In addition, the time series of PRV, LF, HF, LF/HF and PAV were only included when the window size was at least 65s long, as prescribed by HRV analysis standards. Depending on the window, the number of aggregated features in the feature set  $\mathbf{F}$  was  $2 \times 69 = 138$  (if window  $< 65$ s) or  $2 \times 74 = 148$  (if window  $\geq 65$ s).

### 2.3. Feature Selection and Classification

The set  $\mathbf{F}$  was derived from the evening PPG (pre-sleep,  $\mathbf{F}_{\text{pre}}$ ) and morning PPG (post-sleep,  $\mathbf{F}_{\text{post}}$ ). Patients with presence of risk factors for CVD (hypertension, hyperlipidemia or diabetes) were grouped as CVD, and Non CVD otherwise. Next, feature selection and classification was performed over a stratified 10-fold cross validation, repeated 100 times. This was done separately for  $\mathbf{F}_{\text{pre}}$  and  $\mathbf{F}_{\text{post}}$ . Within the training subjects, features were individually normalized by subtracting the mean and dividing by the SD of the feature. Normalized features with a Spearman correlation higher than 0.50 with age or BMI, or higher than 0.90 with other features, were removed. The Minimum Redundancy Maximum Relevance (mRMR) algorithm ranked the remaining features. Within every fold, the top three features received one vote. Thus, the selection frequency of a feature was its percentage of votes over 10 folds and 100 iterations. The Mann-Whitney U-test (with  $p < 0.05$ ) assessed the discriminatory power of the most voted features to separate Non CVD from CVD. In addition, the top three features trained a Naive Bayes (NB), k-Nearest Neighbors (kNN) and Support Vector Machine (SVM) classifier. The mRMR-selected features of the validation subjects of the fold were normalized using the same mean and SD as the training set, and were subsequently fed to the trained classifiers. The performance was assessed by the Cohen’s Kappa score  $\kappa$  over all subjects after cross validation and averaged over 100 iterations.

### 3. Results

The selection frequencies of the four most voted features from pre-sleep PPG data are visualized in figure 2a. The mean diastolic width at 10% of pulse amplitude (mean DT 10%) was most voted for all window sizes, with a frequency ranging between 96.1% and 99.8%. The boxplot of mean DT 10% for non CVD and CVD patients for a 5s window is displayed in figure 2b. The diastolic width at

baseline (mean DT 0%) was the second most voted feature for 5s to 55s (figure 2c). Both features were significantly different for non CVD and CVD patients for all window sizes. For larger windows (65s to 85s), the mean PRV was the second most voted feature, but did not result in significant different patient distributions.

For post-sleep PPG, the mean slope over 5s to 35s was most voted with a selection frequency between 77.6% and 95.1%, and was significantly different for non CVD and CVD. Other highly selected features were the mean DT 0% and mean DT 10%. The latter was significantly different for non CVD and CVD for all window sizes.

CVD classification reached the highest performance for pre-sleep PPG features in combination with an SVM classifier. Using the top three features in every fold, the average  $\kappa$  value had a range between 0.41 and 0.46 for windows of 5s to 55s, with an optimum at 45s ( $\kappa = 0.46 \pm 0.04$ ). In the analysis using 45s windows,  $9.4\% \pm 1.5\%$  of features were confounded with age or BMI. After removing those,  $77.5\% \pm 1.5\%$  of features were highly correlated to other features, and were removed as well. This resulted, on average, in 32 out of 138 remaining features. The CVD classification reached a mean sensitivity of 72.1%, mean specificity of 74.3% and mean accuracy of 73.1%.

### 4. Discussion

This study investigated the PPG waveform in pre- and post-sleep data to characterize CVD risk factors. In evening data, a decrease in diastolic width (at 0% and at 10% of pulse amplitude) and pulse width were indicative for CVD patients. Indeed, the pulse width was shown to provide information on cardiac and arterial dynamics. In [3], it was found that the pulse width was sensitive to changes in systemic vascular resistance, which in its turn is modulated by changes in blood vessel diameters and blood viscosity. In addition, the pulse width reflects changes in pulse wave velocity [3, 9]. Hence, this study confirmed that a patient’s cardiovascular condition is reflected in the PPG wave morphology. However, further studies need to investigate the different modulating factors.

Overall, the mean DT 10% was the most distinctive feature for CVD risk detection. Based on the Mann-Whitney U-test, the feature separated CVD from non-CVD using pre- and post-sleep PPG and all window sizes. This demonstrated the discriminative power of this feature, as well as its robustness. On the other hand, the mean PRV was included in  $\mathbf{F}_{\text{pre}}$  and  $\mathbf{F}_{\text{post}}$  for windows larger than 65s and was the second most voted feature by mRMR. However, the feature could not separate CVD from non CVD and resulted in inferior  $\kappa$  scores in combination with other features such as the mean DT 10%.

The classification performance was maximal for features of  $\mathbf{F}_{\text{pre}}$  analyzed over a 45s window. However, the number of patients in the dataset should be expanded in order to validate this result. In addition, it is desired to repeat the experiments using wearable PPG data. For this, a window of 5s is proposed for data analysis as with short

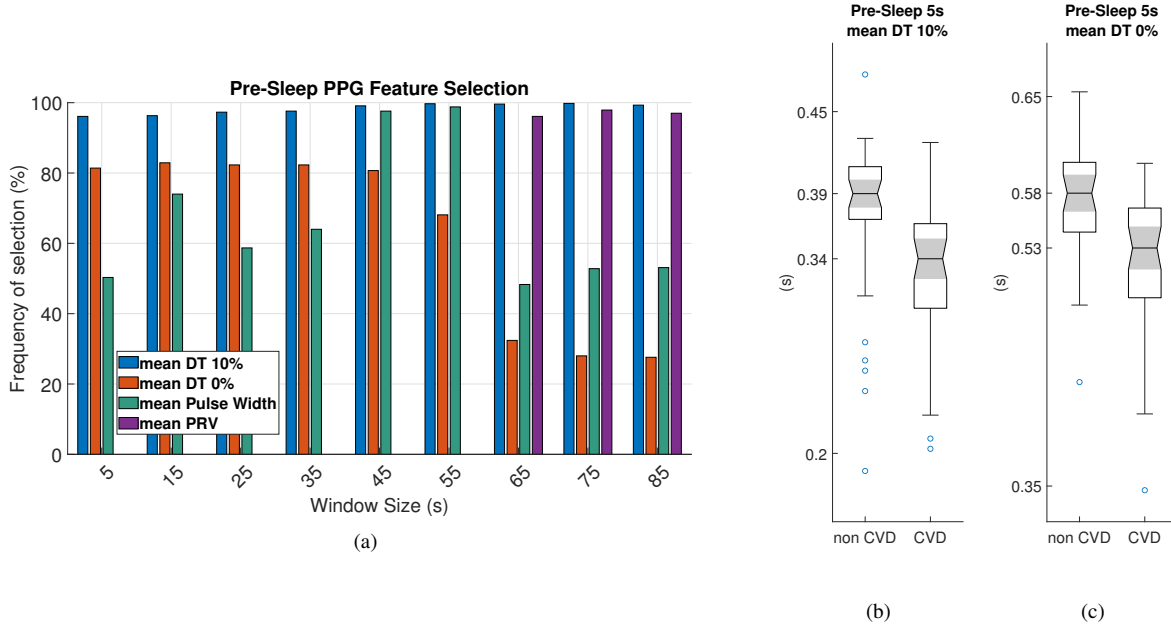


Figure 2: Most voted PPG features for CVD risk detection derived from pre-sleep data. (a) Frequency of feature selection over 100 iterations and 10-fold cross validation. (b) Mean diastolic width at 10% of the pulse amplitude and (c) at baseline.

intervals the minimal recording time in a patient can be decreased. In addition, the method becomes applicable on data with occasional artefacts, as only small data windows around the artefact need to be removed. This enables the application on wearable data, which is typically sensitive to movement artefacts. The use of 5s windows is supported by the results of this study as the classification performance using 5s was similar to 45s.

## 5. Conclusions

The mean DT 10% showed a significant decrease for CVD patients, both in pre-sleep and post-sleep PPG. The combination with two other pulse width related features of pre-sleep PPG resulted in a CVD risk detection with  $\kappa = 0.46$ . This approach could aid to prioritize patients for sleep apnea diagnosis and treatment, in order to avert development of aggravating CVD. However, a validation on larger datasets and wearable sensors is required. For the latter, an analysis using short 5s windows was proposed to account for artefact sensitive PPG.

## Acknowledgements

Agentschap Innoveren en Ondernemen (VLAIO) 150466: OSA+ ; Flemish Government: This research received funding from the Flemish Government (AI Research Program). Sabine Van Huffel and Dorien Huysmans are affiliated to Leuven.AI - KU Leuven institute for AI, B-3000, Leuven, Belgium.

## References

- [1] Ucak S, et al. Heart rate variability and obstructive sleep apnea: Current perspectives and novel technologies. *Journal of Sleep Research* 2021;e13274.
- [2] Linder SP, et al. Using the morphology of photoplethysmogram peaks to detect changes in posture. *J Clin Monit Comput* ;20(3):151–158.
- [3] Awad AA, et al. The relationship between the photoplethysmographic waveform and systemic vascular resistance. *J Clin Monit Comput* 2007;21(6):365–372.
- [4] Kurylyak Y, et al. A neural network-based method for continuous blood pressure estimation from a ppg signal. In *I2MTC*. IEEE, 2013; 280–283.
- [5] Ramachandran D, et al. Computerized approach for cardiovascular risk level detection using photoplethysmography signals. *Measurement* 2020;150:107048.
- [6] Lázaro J, et al. Pulse rate variability analysis for discrimination of sleep-apnea-related decreases in the amplitude fluctuations of pulse photoplethysmographic signal in children. *IEEE J Biomed Health Inform* 2013;18(1):240–246.
- [7] Lázaro J, et al. Pulse photoplethysmography derived respiration for obstructive sleep apnea detection. In *CinC*. IEEE, 2017; 1–4.
- [8] Deviaene M, et al. Sleep apnea detection using pulse photoplethysmography. In *CinC*, volume 45. IEEE, 2018; 1–4.
- [9] Arza A, et al. Pulse transit time and pulse width as potential measure for estimating beat-to-beat systolic and diastolic blood pressure. In *CinC*. IEEE, 2013; 887–890.

Address for correspondence:

Dorien Huysmans  
 ESAT/STADIUS/KU Leuven  
 Kasteelpark Arenberg 10, bus 2446, 3001 Leuven, Belgium  
 dorien.huysmans@esat.kuleuven.be